Perturbed angular correlation characterization of indium species on In/H-ZSM5 in the presence of water and catalytic deactivation studies during the SCR of NO_x with methane

J.M. Ramallo-López [a,*], L.B. Gutierrez [b], A.G. Bibiloni [a], F.G. Requejo [a,†], and E.E. Miró [b]

[a] *Instituto de Física de La Plata (CONICET), Dep. de Física, Fac. Ciencias Exactas, UNLP CC/67 1900 La Plata, Argentina*
[b] *Instituto de Investigaciones en Catálisis y Petroquímica, INCAPE (CONICET), Fac. Ingeniería Química, UNL*
Santiago del Estero 2829, 3000 Santa Fe, Argentina

Received 21 March 2002; accepted 7 May 2002

An In(4 wt%)-impregnated H-ZSM5 catalyst was characterized under wet and dry conditions by time-differential perturbed angular correlation (PAC) and by temperature-programmed reduction (TPR). Different indium species were quantified, correlating their structure with the catalyst deactivation due to the presence of water during the NO selective catalytic reduction (SCR) with methane. The fresh sample contains ~60% of indium oxide and 40% of $(InO)^+$ species at exchange sites, the latter being the active species for the reaction under study. Under wet atmosphere, hyperfine interactions determined by PAC indicate the formation of two types of In hydroxide species and the decrease of both $(InO)^+$ and In_2O_3. TPR and PAC characterizations also show that deactivation is due to the decrease of $(InO)^+$ at exchange sites to form, after water is removed, different non-active In oxide species.

KEY WORDS: environmental chemistry; nitric oxide abatement; In/H-ZSM5; PAC.

1. Introduction

The selective catalytic reduction of NO_x using methane instead of ammonia proceeds even in the presence of excess oxygen on some metal-exchanged zeolites such as Co ion-exchanged ZSM5 and ferrites [1,2], Ga ion-exchanged ZSM5 [3], and In ion-exchanged ZSM5 [4]. Ga-ZSM5 exhibits a high selectivity of NO reduction; however, its activity is strongly suppressed by the presence of water [5]. Kikuchi and co-workers [6–8] have recently reported that In-ZSM5 has higher SCR activity in the presence of water than Ga-ZSM5 and that the addition of a noble metal such as Pt, Rh or Ir greatly improves the water tolerance of the catalyst. It has been suggested that the activity of In-ZSM5 catalysts for the SCR reaction is due to the presence of $(InO)^+Z^-$ groups [8]. It has been proposed that these groups, in the presence of water, be coordinated with water molecules forming $[In(OH)_2]^+Z^-$ species, poisoning the ability of indium for the NO_2 adsorption step, which is known to be essential [8]. Zeolite acid sites, active for the NO oxidation to NO_2, are also inhibited due to water adsorption. Thus, it is indicated that substitution for these Lewis acid sites, on which NO oxidation proceeds, is effective in order to improve the catalytic performance in the presence of water vapor. In fact, the precious-metal loaded In/H-ZSM5 shows high catalytic activity for NO reduction with CH_4 even in the presence of water vapor [8].

In previous works we have reported the first perturbed angular correlation (PAC) characterization technique of In species in SCR catalysts [9,10], identifying the active species for the reaction and following its evolution under reduction/oxidation treatments. The main species identified were In_2O_3 (indium sesquioxide crystals), In^+Z^- and $(InO)^+Z^-$ (different indium species exchanged in the zeolitic matrix), and highly dispersed non-crystalline In oxide species not bonded to the zeolite matrix. Impregnated catalysts, followed by calcination at 500 °C, had low activity for the reduction of NO with CH_4 in the presence of excess oxygen, showing only In_2O_3 and non-crystalline In oxide species. Treatments at 750 °C in O_2, or at 500 °C in H_2, followed by re-oxidation at the same temperature resulted in active catalysts showing an appreciable concentration of $(InO)^+Z^-$ active species. Nevertheless, in these previous studies, we have only characterized the active In sites under air (room) conditions.

Because of its capabilities, the time-differential PAC technique is a prominent characterization tool for catalytic systems as it allows *in-situ* studies of dispersed and diluted (as low as ppm) phases in catalysts [11,12]. Through the measure of the angular correlation of two gamma rays emitted by a radioactive probe, the technique permits the determination of the electric field gradient (EFG) at the probe site. From this, information

---

[*] To whom correspondence should be addressed.
[†] Present address: Materials Science Division, LBNL, Mailstop 66-200, Berkeley, CA 94720, USA.

1011-372X/02/0900-0131 © 2002 Plenum Publishing Corporation

about the characteristics (coordination, symmetry, distortions, etc.) of the different environments of the radioactive probes, their concentrations and modifications related to *in-situ* conditions can be obtained. This is possible by means of the hyperfine interaction between the nucleus of the probe and the EFG produced by the extranuclear (ion and electronic) charges [13]. As the technique requires the detection of γ-rays, which penetrate matter very easily with practically no absorption, PAC is especially suitable for *in-situ* experiments, allowing performance of experiments at room temperature and with flowing gases through the sample. A brief and clear description of this technique and of the typical equipment set-up was published by Vogdt *et al.* [14]. The technique has been applied by our group to the catalyst field for some years, particularly in the identification of Mo species on supported catalysts [15,16]. In the case of In-supported catalysts, the time-differential observations of the perturbed angular correlation of γ-rays emitted from radioactive ^{111}In (probe) allowed the characterization of different In sites (and In species). Since the EFG depends on r^{-3} (where r is the distance between the probe and the charge), the PAC technique is a local-environment characterization technique. Then, the PAC experiments are very appropriate for characterizing species with different local environment and/or short-range order (as in the case of species exchanged in zeolites).

In this work we present a series of PAC, temperature-programmed reduction (TPR) and kinetic experiments performed under controlled dry and wet atmospheres in order to study the nature of the active species for the SCR of NO in an In/H-ZSM5 impregnated catalyst in different conditions. In particular we discuss the effect of water on the characteristics of the interaction of $(InO)^+Z^-$ (active sites for the SCR of NO) and In_2O_3 species with the water present in the reactor feed.

2. Materials and methods

2.1. Catalyst preparation

A commercial Na-ZSM5 zeolite (Chemie Uetikon, PZ-2/54 Na) with a chemical Si/Al ratio of 26.4, determined by chemical analysis, was the starting material. The ammonium form was prepared by ionic exchange using an aqueous solution of NH_4NO_3 (1 M), with a zeolite/solution ratio of $3\,g\,l^{-1}$ at reflux temperature (~100 °C), for 24 h. The degree of ionic exchange was determined by atomic absorption, being higher than 99% of the ionic exchange capacity.

Indium was incorporated to the zeolite using the conventional wet impregnation method, stirring an aqueous solution of $InCl_3$ and NH_4-ZSM5 at 80 °C until all water was evaporated, followed by drying in a stove at 120 °C for 12 h. After that, the solid was pretreated in a dry oxygen atmosphere by heating up to 500 °C at 5 °C/min, and holding the final temperature for 12 h (standard calcination procedure). In this way, samples with 4 wt% of In were obtained. The pore volume of these samples was $0.11\,cm^3/g$ and it was measured by nitrogen adsorption at 77 K and at $P/P^0 = 0.5$. After the standard calcination procedure, the samples were calcined for 2 h in oxygen at 750 °C. During this high-temperature treatment $(InO)^+$ active sites were formed through the reaction of different In oxide species and acid sites [10]. In order to perform PAC experiments, the probe (^{111}In) was introduced by adding traces of $^{111}InCl_3$ to the non-radioactive $InCl_3$ solution.

2.2. Catalytic measurements

The reaction was carried out using 0.5 g of catalyst placed on a tubular quartz fixed-bed flow reactor, 12 mm i.d. The typical reacting mixture consisted of 1000 ppm of CH_4, 1000 ppm of NO and 10% of O_2 balanced at 1 atm with He (GHSV: $6500\,h^-1$ referred to the same total weight of the catalysts). Water was introduced through a distilled-water saturator carefully thermostat-controlled at different temperatures, in order to obtain 2, 8, 15 and 30 vol% of water in the gaseous feed.

The catalytic activity was measured with an SRI 9300B chromatograph with two columns, 5 Å molecular sieve and Chromosorb 102. The NO_x conversion (C_{NO_x}) was calculated from N_2 production: $C_{NO_x} = 2[N_2]/[NO]^\circ \times 100$, where $[NO]^\circ$ is the NO concentration in the feed. The CH_4 conversion (C_{CH_4}) was obtained as $C_{CH_4} = ([CH_4] - [CH_4]^\circ)/[CH_4]^\circ) \times 100$.

2.3. Catalyst characterization

2.3.1. TPR experiments

These were performed with 100 mg of catalyst using an Okhura TP-2002 S instrument equipped with a TCD detector. The reducing gas was 5% H_2 in Ar and the heating rate was 10 °C/min.

2.3.2. PAC measurements

The PAC technique rests on the fact that, due to the conservation of angular momentum, the direction of emission of a photon in a nuclear decay is strictly correlated with the orientation of the nuclear spin [13]. Then, in a radioactive source with the nuclei randomly oriented, it is possible to select a set of nuclei with a particular spin orientation detecting the first radiation γ_1 of a γ–γ cascade in a fixed direction $\vec{\mathbf{k}}_1$. The detection of the second γ-ray, γ_2, will therefore show a certain angular distribution pattern with respect to the direction $\vec{\mathbf{k}}_1$. The density of probability $W(\theta, t)$ of the second emission in the direction $\vec{\mathbf{k}}_2$, detected at an angle θ with respect to $\vec{\mathbf{k}}_1$, will be perturbed if, during the time t the nuclei remain in the intermediate level, interaction with extranuclear fields occurs. Thus, $W(\theta, t)$ is written as [13]:

$$W(\theta, t) = 1 + A_{22}G_{22}(t)P_2(\cos\theta), \quad (1)$$

where A_{22} is the anisotropy of the cascade that depends only on nuclear properties, and $P_2(\cos\theta)$ is the second-order Legendre polynomial that reflects the angular dependence of $W(\theta, t)$. Higher terms in equation (1) are negligible in the case of the ^{111}Cd cascade due to the small values of the A_{22} coefficients. In the absence of magnetic fields, the perturbation function $G_{22}(t)$ contains all the information of the hyperfine interactions between nuclear electric quadrupole moment eQ with an extranuclear EFG. This EFG results from the charge-density distribution, which, in turn, depends on the electric characteristics of the atomic surroundings and on the nature of the chemical bonds.

For polycrystalline samples and a nuclear spin $I = 5/2$ of the intermediate nuclear level of the cascade, the perturbation factor $G_{22}(t)$ for static electric quadrupole interactions has the following form [13]:

$$G_{22}(t) = \sum_i f_i\left(S_{20,i} + \sum_{n=1}^{3} S_{2n,i}\cos(\omega_{ni}t)\,\mathrm{e}^{-\delta_i\omega_{ni}t}\right) \quad (2)$$

where f_i is the relative fraction of nuclei that experiences a given perturbation. The ω_n frequencies are related to the quadrupole frequency $\omega_Q = eQV_{ZZ}/40\hbar$ by $\omega_n = g_n(\eta)\omega_Q$. The g_n and S_n coefficients are known functions [17] of the asymmetry parameter $\eta = (V_{YY} - V_{XX})/V_{ZZ}$, where V_{ii} is the principal component of the EFG tensor and $|V_{XX}| < |V_{YY}| < |V_{ZZ}|$. The exponential functions account for a Lorentzian frequency distribution of relative width δ around ω_n.

A four BaF-detector fast–fast coincidence system in a coplanar arrangement, with a time resolution of 1 ns, was used to perform the PAC experiments. All experiments were performed at 500° C in order to avoid electronic relaxation phenomena, also known as "after effect", produced by the electron capture decay of the $^{111}\mathrm{In} \to {}^{111}\mathrm{Cd}$ [18,19]. Eight coincidence spectra (four at 90° and four at 180°) of all possible start–stop combinations of the four detectors were simultaneously recorded in a multichannel analyzer. The coincidence $C_{ij}(t)$ is the result of the detection of the two γ-rays from a double cascade decay coming from the same nucleus in detectors i and j separated by an angle of θ degrees with an interval of t sec between them. From the coincidences at two angles (90° and 180°) these two relations can be constructed:

$$W(180^\circ, t) = [C_{13}(t) + C_{31}(t)]^{1/2}[C_{24}(t) + C_{42}(t)]^{1/2} \quad (3)$$

and

$$W(90^\circ, t) = [C_{12}(t) + C_{21}(t)]^{1/2}[C_{34}(t) + C_{43}(t)]^{1/2} \quad (4)$$

Finally, the asymmetry ratio $R(t)$ becomes:

$$R(t) = 2\frac{[W(180^\circ, t) - W(90^\circ, t)]}{W(180^\circ, t) + 2W(90^\circ, t)} \approx A_{22}^{\mathrm{exp}}G_{22}(t), \quad (5)$$

where A_{22}^{exp} is the effective anisotropy of the cascade for certain experimental conditions.

Performing a non-square fit of the theoretical perturbation factor $A_{22}^{\mathrm{exp}}G_{22}(t)$ to this $R(t)$ spectrum, the hyperfine parameters (relative concentration f, quadrupole frequency ω_Q, asymmetry parameter η, and distribution percentage δ) for each probe's inequivalent site can be obtained.

3. Results

3.1. Kinetic studies

In a recent paper, we reported on a detailed characterization of the state of indium in In/H-ZSM5 catalysts [10]. The main species identified were In_2O_3 (indium sesquioxide crystals), In^+Z^- and $(InO)^+Z^-$ (different indium species exchanged in the zeolitic matrix), and highly dispersed non-crystalline In oxide species not bonded to the zeolite matrix. The distribution of the different species, and the catalytic activity, strongly changes with catalyst preparation and pretreatment procedures. For example, impregnated catalysts, followed by calcination at 500 °C, had low activity for the reduction of NO with CH_4 in the presence of excess oxygen, showing only In_2O_3 and non-crystalline In oxide species. Treatments at 750 °C in O_2, or at 500 °C in H_2 followed by re-oxidation at the same temperature resulted in active catalysts showing an appreciable concentration of $(InO)^+Z^-$ active species [10]. Nevertheless, in these studies, we have only characterized the active In sites under air (room) atmosphere. Since, under practical conditions, the presence of water is unavoidable, and it is readily known that it negatively affects the catalytic behavior of In zeolite catalysts, we focused this work on the characterization of In species under a controlled wet atmosphere.

Figure 1 shows the catalytic results for In-impregnated H-ZSM5 catalysts with different pretreatments. As mentioned before, this catalyst presents a reasonable activity only after reduction at 500 °C or calcination at 750 °C, the latter treatment being the more effective. In the same figure, it can be seen that the presence of 2 vol% of water in the feed decreases the catalytic activity and that, after water is removed from the feed, the original activity is restored. The following results presented in this paper were all performed with a 4 wt% In/H-ZSM5 impregnated catalyst, followed by calcination at 750 °C.

Figure 2 shows the effect of water on nitric oxide conversions at 450 °C and 500 °C. It can be seen that the nitric oxide conversion steadily decreases between 0 and 30 vol% of water. In the same figure we can see that, while at low water-content in the feed the activity

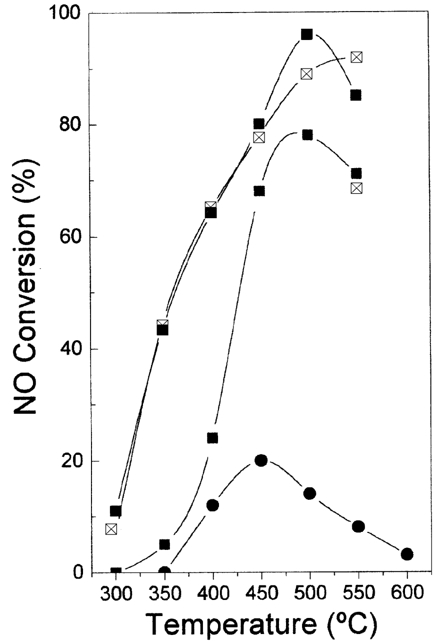

Figure 1. SCR of NO on In(4%)-H-ZSM5. Pretreatment effect on NO conversion. ● Calcined at 500 °C, ■ calcined at 750 °C. Reaction conditions: GHSV: 6500 h^{-1}, [NO] = [CH$_2$] = 1000 ppm, [O$_2$] = 2%, [H$_2$O]%. Closed symbol: dry conditions, open symbol: wet conditions, crossed symbol: after water was removed from the feed stream.

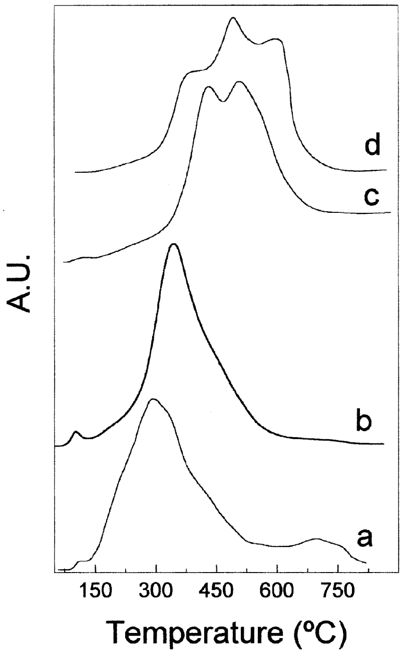

Figure 3. TPR profiles of In(4%)-H-ZSM5 after different treatments. (a) Fresh, calcined at 750 °C, (b) used under wet reaction conditions (8% H$_2$O), (c) used under wet reaction conditions (30% H$_2$O), (d) severe treatment (900 °C reached in 30 min under oxygen stream).

is restored when water is removed, at water contents above 15% an irreversible decrease in activity takes place. This activity loss could not be overcome with another calcination at 750 °C. Since the irreversible deactivation must involve some structural changes in active sites, we characterized the catalyst at hand by TPR and PAC techniques under both dry and wet atmospheres.

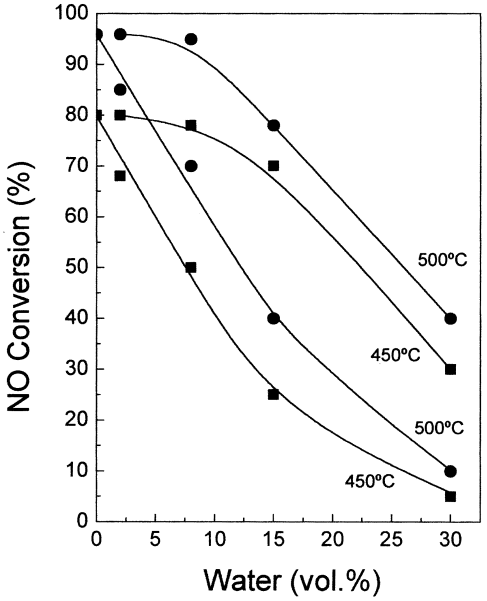

Figure 2. Effect of water content on the SCR of NO$_x$. In(4%)-H-ZSM5 catalyst calcined at 750 °C. Closed symbols: with different amounts of water in the feed. Open symbols: after water was removed from the feed. Reaction conditions: see figure 1 legend.

3.2. Catalyst characterization

To gain insight into the deactivation phenomenon, different pretreated samples were characterized with the TPR technique and results are shown in figure 3. It can be observed that, for the In (4%) impregnated sample calcined at 750 °C, a reduction zone between 200 and 500 °C exists, centered at approximately 300 °C (figure 3(a)). It has been previously reported [10] that the reduction process mainly consists of two reactions: $(InO)^+Z^- + H_2 = In^+Z^- + H_2O$ and $In_2O_3 + 2H^+Z^- + H_2 = 2In^+Z^- + 3H_2O$. In figure 3(a), two non-resolved peaks can be seen that correspond to the mentioned reactions, and also a small higher-temperature peak due to the reduction of some amount of bulk In_2O_3. The reduction main signals suffer a small shift to higher temperatures in the sample that has been treated under reaction conditions with 15% water (figure 3(b)). The observed signal shift is more pronounced when the sample has been treated under reaction with 30 vol% of water (figure 3(c)).

The TPR curve in figure 3(d) corresponds to a sample with a severe pretreatment. This pretreatment was performed after the impregnation and drying procedure at 120 °C, and consisted of quickly heating up from room temperature to 900 °C (in approximately 30 min). In this sample, the presence of In sesquioxide crystals was verified by XRD, and the TPR looks shifted to

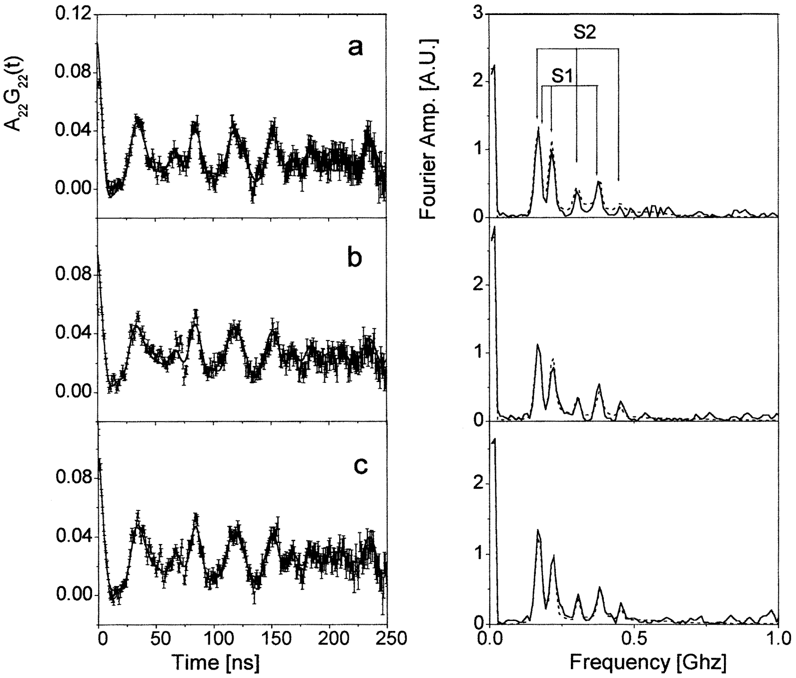

Figure 4. PAC spectra (left) and their corresponding Fourier transforms (right) of In/H-ZSM5 taken at 500 °C in three different atmospheres: (a) vacuum, (b) air and (c) N_2 flux. Inset in Fourier transforms indicates the three hyperfine interactions for S1 and S2 signals.

higher temperatures if compared with that of figure 3(c). In all cases, the hydrogen consumption during TPR lay between 0.9 and 1.2 mol of H_2 per mol of In, the stoichiometric ratio being 1.0 for $(InO)^+$ species and 1.5 for In_2O_3.

In order to study the characteristics of the active indium sites and the interaction of indium species with water molecules in the In/H-ZSM5 catalyst, PAC experiments in different conditions were performed. Up to now we have only characterized the catalysts under room conditions. Next we try to examine the effect of different atmospheric conditions on these indium sites, and in particular the effect of water vapor on active sites. Figure 4 shows PAC spectra taken at 500 °C in three different atmospheres: (a) vacuum, (b) air and (c) N_2 flux for In/H-ZSM5. Figure 5 shows the spectra in (a) N_2 + 15% of H_2O flux and (b) in N_2 after this treatment. Their corresponding Fourier transforms are also shown in the figures on the right. The solid line corresponds to the fitted function $R(t)$ for each spectrum. In table 1, the corresponding hyperfine parameters f, ω_Q, η and δ obtained from fitting formula (5) to the experimental data are shown.

The PAC spectra for the fresh sample in vacuum, in N_2 and in air show a similar behavior (figures 4(b) and 4(c)). In effect, the hyperfine parameters of these samples

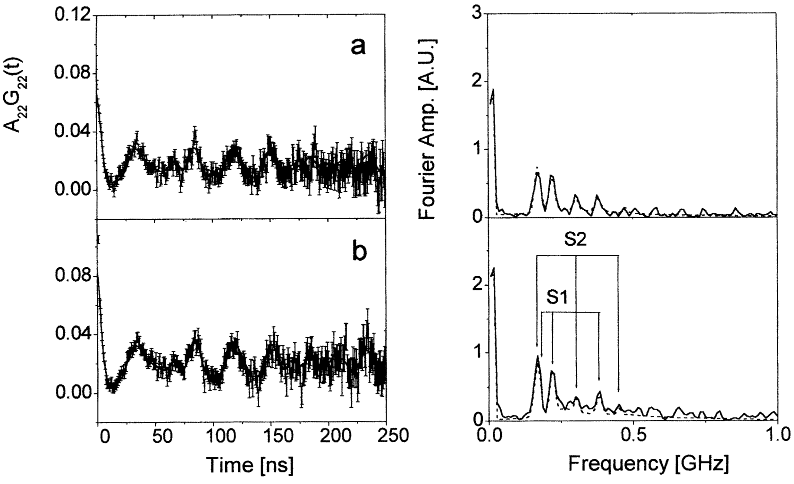

Figure 5. PAC spectra (left) and their corresponding Fourier transforms (right) of In/H-ZSM5 taken at 500 °C (a) in N_2 + 15% of H_2O and (b) in N_2 after this treatment. Inset in Fourier transforms indicates the three hyperfine interactions for S1 and S2 signals.

Table 1
Hyperfine parameters obtained for the catalyst In/ZSM5 in the conditions stated

Conditions	Population (%)	Frequency ω_Q (MHz)	Asymmetry parameter η	Distribution δ (%)	Site label
Vacuum	47 (5)	18.9 (1)	0.70 (3)	0.8 (2)	S1
	14 (2)	24.7 (1)	0.06 (4)	0.0	S2
	39 (5)	28.1 (8)	0.30 (5)	14 (2)	S3
Air	47 (5)	18.9 (1)	0.70 (2)	1.6 (4)	S1
	12 (3)	24.8 (1)	0.05 (3)	0.1 (1)	S2
	41 (4)	34 (2)	0.3 (1)	29 (5)	S3
N_2	41 (7)	19.1 (1)	0.69 (1)	0.7 (3)	S1
	13 (2)	24.8 (1)	0.03 (2)	0.0	S2
	46 (4)	29.7 (8)	0.0	19 (3)	S3

All measures were performed at 500 °C. Corresponding spectra are shown in figure 4.

show the existence of three different sites for indium probes. The first two, labeled S1 and S2, correspond to those found for indium sesquioxide in a 3:1 ratio, which has been extensively studied with this technique [19–21]. There is a slight increase in their distribution parameters in the sample measured in air, which is evident in the height of the principal peaks in the Fourier transforms. The third site, labeled S3, corresponds to the parameters assigned to the active sites for the SCR of NO $(InO)^+Z^-$ [10] and are the same for the measurements in vacuum and N_2 flux, while, as happened for the sites corresponding to In_2O_3, the distribution increases for the measure in air. The rest of the parameters remain unchanged in the three samples. That is, in the fresh catalyst, 60% of the indium atoms are forming indium sesquioxide while the rest are at exchange cationic sites.

When the catalyst is exposed to a flux of N_2 and 15% of H_2O (figure 5(a) and table 2) there is a change in the hyperfine parameters fitted to the spectra. The two sites corresponding to indium sesquioxide are still present but their populations have diminished. In contrast, the population of the third interaction is greater than in the measurement in air and its hyperfine parameters have changed. This may be indicating an increase in the number of indium atoms in exchange sites, but their hyperfine interactions are different from that corresponding to the active site. It should be remarked that the distribution percentage of this species is greater than that corresponding to the active site in dry conditions, indicating a big inhomogeneity in the site configuration. When the addition of water is stopped from the feed stream and the sample is measured in air again, there is a decrease of the population of the third site and their parameters change once more, but those corresponding to the active site are not completely recovered, thus indicating a non-reversible process.

4. Discussion

Recently, the selective reduction of NO with hydrocarbons in the presence of oxygen excess using metal-exchanged zeolites has been widely investigated as a promising technique for solving the problem of NO_x emissions in both stationary and mobile sources. However, the severe deactivation that metal zeolites suffer due to the presence of water poses a limitation in the possibilities for its use under practical conditions. This deactivation problem has been addressed by several authors. Kharas *et al.* [22,23] studied the deactivation of the Cu-ZSM5 catalyst. They observed the formation of CuO in catalytically or hydrothermally deactivated catalysts but not in fresh catalysts by XRD, and high-resolution TEM revealed a loss of crystallinity of the zeolite in thin regions of the exterior surfaces of zeolite crystal grains [22]. They proposed that two phenomena

Table 2
Hyperfine parameters obtained for the catalyst In/ZSM5 in the conditions stated

Conditions	Population (%)	Frequency ω_Q (MHz)	Asymmetry parameter η	Distribution δ (%)	Site label
$N_2 + 15\%\ H_2O$	28 (6)	18.9 (2)	0.67 (1)	1.2 (4)	S1
	8 (2)	25.2 (2)	0.35 (2)	0.5 (3)	S2
	64 (4)	20 (3)	1.0	69 (9)	S4
N_2	36 (8)	19.1 (1)	0.69 (1)	1.2 (3)	S1
	9 (2)	24.7 (2)	0.1 (1)	0.6 (5)	S2
	55 (3)	40 (2)	0.3 (1)	23 (4)	S5

All measures were performed at 500 °C. Corresponding spectra are shown in figure 5.

accompany, and probably cause, catalyst deactivation: the superficial amorphization of the crystalline zeolite, and the sintering of CuO and the resultant local destruction of zeolite crystallinity in the vicinity of sintering oxides of Cu.

Ohtsuka and Tabata [24] studied the effect of water vapor on the deactivation of Pd-zeolite catalysts for the selective catalytic reduction of nitrogen monoxide by methane. They found that Pd–mordenite showed stable activity in the absence of water vapor at 450 °C for more than 30 h, while it showed a gradual decrease in NO_x conversion in the presence of water vapor. They suggested, by using CO adsorption and Raman measurements, that PdO is formed on the deactivated samples, and that the deactivation of Pd-zeolites is caused by Pd agglomeration to form the oxide. Water vapor promotes the agglomeration process.

In this vein, Kikuchi and co-workers [6–8] have recently reported that In/ZSM5 has higher SCR activity in the presence of water than Ga/ZSM5, and that the addition of a noble metal such as Pt, Rh or Ir greatly improves the water tolerance of the catalyst. The authors proposed two inhibition effects: (i) the adsorption of water on zeolite acid sites which inhibits the NO oxidation step, and (ii) the coordination of water molecules to Ga or In sites, forming $[In(OH)_2]^+$ or $[Ga(OH)_2]^+$ species, thus blocking the adsorption of NO_2. The second effect is more pronounced for Ga/H-ZSM5, explaining the higher resistance to water of In catalysts [8]. Thus, it is indicated that substitution for the zeolite Lewis acid sites, on which NO oxidation proceeds, is effective in order to improve the catalytic performance in the presence of water vapor. In/H-ZSM5 loaded with precious metal (Pt, Rh or Ir) shows high catalytic activity for NO reduction with CH_4 even in the presence of water vapor [8].

For our In(4%)/H-ZSM5 impregnated catalyst, we found a reversible deactivation at low contents of water vapor but, under more severe conditions (when the water content is between 15 and 30%) the deactivation is permanent. The reversible process observed at low water content probably originated in the reversible adsorption of water on zeolite acid sites, as suggested by Kikuchi and co-workers [6–8]. The irreversible deactivation observed when the conditions are more severe is most probably due to the decomposition of the active, exchanged sites, to form In oxide species not bonded to the zeolitic matrix. The mechanism of this process would involve the formation of $[In(OH)_2]^+$ species which, after water is removed, are expelled from exchange sites forming In oxide species and/or the loss of the exchange sites that stabilize $(InO)^+$ due to a dealumination under hydrothermal conditions. The XRD patterns of fresh and deactivated catalysts (not shown) are very similar, indicating that the zeolitic structure is not altered, but some local dealumination would occur.

The TPR results are in agreement with this possibility since a temperature shift is observed for catalysts that have been treated under wet reaction conditions. The shift of peaks to a higher temperature is more pronounced for more deactivated catalysts. A catalyst that has been subjected to a severe hydrothermal treatment shows the presence of In sesquioxide in XRD analysis. This is not the case for the catalysts treated under wet reaction conditions, probably because the In oxide particles are small and are not well-defined crystalline structures.

For our fresh In/H-ZSM5 catalyst, the active species $(InO)^+$ are reduced at low temperatures (about 250 °C). The hydrogen consumption in the 300–400 °C temperature range is mainly due to the reduction of well-dispersed indium oxide species not bound to the zeolite matrix [10]. The reduction of these two In species is not resolved in the TPR spectra. In figure 3(a), a small peak at around 700 °C is also observed, probably from the reduction of bulk indium sesquioxide crystals. For the catalysts treated under wet atmosphere (figures 3(b) and 3(c)) the reduction peaks shift to higher temperatures, suggesting the transformations of $(InO)^+$ into extraframework, well-dispersed In oxide species and bulk In sesquioxide. The more severe the treatment, the more shifted to the right the transformation. In the same figure it can be seen that for catalysts treated with 30% water, most of the reduction takes place above 400 °C, only a small proportion (corresponding to $(InO)^+$) being reduced at around 250 °C. The reduction consumption above 400 °C in figure 3(c) shows two peaks, the first being due to the reduction of well-dispersed In oxide species, and the second due to bulk In sesquioxide. In figure 3(d), a third signal appears, probably due to some destruction of zeolite structure associated with the extremely severe treatment and the formation of an In–Al compound. The latter treatment (quickly heating up to 900 °C) was only performed for comparison purposes.

In our previous work [10], we characterized the In species in SCR catalysts by means of the PAC technique, but under air (room) conditions. In the present work, we performed PAC experiments in different atmospheres to characterize and quantify the active species under conditions more similar to those found in reaction conditions and to gain insight about the deactivation phenomenon. As we have shown in section 3, there are no differences in the characteristics of the indium sites in vacuum and in N_2 flux. In both cases indium sesquioxide is found in 60% and the distribution remains unchanged. The characteristics of the active sites are also the same. To simplify the analysis, we shall call these conditions “dry state”. When we compare these results with those found in air (room) conditions, we find only slight differences. Three sets of hyperfine parameters are also fitted. The first two correspond to indium sesquioxide and the third to the active site. Their populations are the same as in vacuum conditions and the only difference in the hyperfine parameters fitted are the distribution percentages. In the results for the measurements in air, the distributions of the three sites are twice those found in dry conditions. This indicates a bigger inhomogeneity in the species. In the case of the In_2O_3 crystals, an increase of the distribution of its sites is commonly associated with a decrease in the size of the crystals. In this case, as no treatment capable of having such an effect is performed on the catalyst, this possibility should be neglected. In effect, neither the vacuum nor the fluxing N_2 may be responsible for producing the sintering of the small oxide crystals found on the external surface of the zeolite. The only effect which these two treatments may have on these crystals is desorption of the gas molecules adsorbed on their surface. In conclusion, the characteristics of the active site of indium for the SCR on NO in the In/H-ZSM5 catalysts found under either vacuum or nitrogen flow conditions are very similar to those found in air (room) conditions in our previous work [10].

Figure 5 shows the effect of water on indium species in the catalysts, indicating changes in the percentages of the species. In effect, a decrease in the quantity of In_2O_3 is found. Moreover, the third species, which corresponds to the active sites, has different parameters from those found before. This change in the parameters of this species indicates a modification of the configuration of the $(InO)^+$ sites, probably because of the absorption of a water molecule and the formation of $[In(OH)_2]^+$ species. The formation of these species would be responsible for the deactivation of the catalyst. The increase in the population of this third hyperfine interaction may be attributed to the existence of a new site which cannot be resolved from $[In(OH)_2]^+$ species because of their distributions. This new site can be produced by the adsorption of water molecules on the indium sesquioxide surface, modifying the electric field gradient on the probes found there. As this effect would not generate well-defined crystal-like structures, their distribution should be very high, explaining the increase found in this parameter for this interaction. Thus, the third interaction in this spectrum (S4) has contributions from two indium species: $[In(OH)_2]^+$ species formed from $(InO)^+$ and from indium at the surface of the sesquioxide crystals. On the other hand, the interaction of In oxide species with extra-lattice aluminum may also contribute to the high distribution observed.

Because In_2O_3 crystallites are not seen by X-ray diffraction, their radii should be smaller than 40 Å. Assuming a radius of 30 Å for our particles, the relation surface atoms/total atoms, calculated using the model proposed by Van Hardeveld and Artog [25], is 0.25. That is, 25% of indium atoms are on the external surface and could adsorb H_2O molecules. As 60% of indium atoms are forming In_2O_3 crystals in our catalyst, 15% of the total atoms are located on the surface of the oxide. Considering that between 40 and 45% of indium atoms should be forming the $[In(OH)_2]^+$ species on the sesquioxide crystal surface, the sum of these sites gives a total between 55 and 60% which, considering the errors of the experimental results, is consistent with the population fitted for S4.

This process is not reversible, as is shown in the parameters found for the sites after water is removed from the feed (figure 5(b) and table 2). After water is removed the parameters for the third site change again but those of $(InO)^+$ at exchange sites are not recovered. This confirms that water has a permanent effect on indium species, destroying the active sites for the SCR of NO, and explains the irreversible deactivation observed after this treatment.

5. Conclusions

Catalytic experiments show a reversible deactivation, which takes place at low water contents, and an irreversible one under more severe conditions. TPR and PAC characterizations suggest that the irreversible deactivation is due to the destruction of $(InO)^+$ at exchange sites to form non-active In oxide species, similar to the behavior reported for other systems such as Cu and Pd zeolites [22–24].

PAC characterization also shows that the characteristics of the indium species found in In/HZSM5 under vacuum are similar to those found in air or nitrogen, the only slight difference being a better definition of sites in the former case. This is true both for indium sesquioxide and for the active sites $(InO)^+Z^-$.

When concentrations of 15% of water are added, changes on the characteristics of the indium species present in the catalyst are seen, and active sites are irreversibly destroyed. This effect possibly takes place because of the coordination of water molecules to form In hydroxide species which, when dehydrated, do not restore the active species. PAC characterization suggests two types of hydroxide species, one formed from the interaction of water with $(InO)^+$, and the other from the interaction of water with In atoms located at the surface of sesquioxide crystals.

Acknowledgments

The authors are grateful to Agencia de Promoción a la Investigación (proy. PICT 14-6971), UNL (CAI + D ’96 Program) and CONICET, Argentina, through grant PEI-0132/98. Thanks are also given to Ing. Jorge Runco for his technical assistance in the experimental PAC set-up, and to Elsa Grimaldi for the editing of the English manuscript.

References

[1] Y. Li, and J.N. Armor, US Patent 5,149,512 (1992).

[2] Y. Li, and J.N. Armor, Appl. Catal. B 1 (1992) L31.

[3] K. Yogo, M. Ihara, I. Terasaki and E. Kikuchi, Chem. Lett. (1993) 229.

[4] E. Kikuchi and K. Yogo, Presented at the International Forum on Environmental Catalysis '93, Tokyo, Japan, 4–5 February 1993.

[5] Y. Li and J.N. Armor, J. Catal. 145 (1994) 1.

[6] E. Kikuchi and K. Yogo, Catal. Today 22 (1994) 73.

[7] E. Kikuchi, M. Ogura, N. Aratani, Y. Sugiura, Hiramoto and K. Yogo, Catal. Today 27 (1996) 35.

[8] M. Ogura, M. Hayashi and E. Kikuchi, Catal. Today 42 (1998) 159.

[9] J.M. Ramallo López, F.G. Requejo, M. Rentería, A.G. Bibiloni and E.E. Miró, Hyp. Int. 120/121 (1999) 529.

[10] E.E. Miró, L. Gutierrez, J.M. Ramallo and F.G. Requejo, J. Catal. 188 (1999) 375.

[11] F.G. Requejo and A.G. Bibiloni, Phys. Status Solidi A 148 (1995) 497.

[12] F.G. Requejo and A.G. Bibiloni, Langmuir 12(1) (1996) 51.

[13] H. Frauenfelder and R.M. Steffen, in: *Alpha-, Beta- and Gamma-Ray Spectroscopy*, Vol. 2, ed. K. Siegbalni (North-Holland, Amsterdam, 1968), p. 997.

[14] C. Vogdt, T. Butz, A. Lerf and H. Knözinger, J. Catal. 116 (1989) 31.

[15] A.J. Marchi, E.J. Lede, F.G. Requejo, M. Rentería, S. Irusta, E.A. Lombardo and E.E. Miró, Catal. Lett. 48 (1997) 47.

[16] S. Irusta, F.G. Requejo, E.A. Lombardo and E.E. Miró, Lat. Am. Appl. Res. 24 (1994) 187.

[17] L.A. Mendoza-Zélis, A.G. Bibiloni, M.C. Caracoche, A. López García, J.A. Martínez, R.C. Mercader and A.F. Pasquevich, Hyp. Int. 3 (1977) 315.

[18] A.G. Bibiloni, C.P. Massalo, J. Desimoni, L.A. Mendoza Zelis, F.H. Sánchez, A.F. Pasquevich, L. Damante and A.R. López García, Phys. Rev. B 32 (1985) 2393.

[19] S. Habenicht, D. Lupascu, M. Uhrmacher, L. Ziegeler, K.P. Lieb, and SOLDE Collaboration, Z. Phys. B 101 (1996) 187.

[20] J. Desimoni, A. Bibiloni, L. Mendoza Zelis, A. Pasquevich, F. Sánchez and A. López García, Phys. Rev. B 28 (1983) 5739.

[21] A. Bartos, K.P. Lieb, A.F. Pasquevich and M. Uhrmacher, Phys. Lett. A 157 (1991) 513.

[22] K.C. Kharas, D.J. Liu and H.J. Robota, Appl. Catal. B 2 (1993) 225.

[23] K.C. Kharas, H.J. Robota and A. Datye, in: *Environmental Catalysis*, ed. J.N. Armor, American Chemical Society Symposium Series, Vol. 552 (American Chemical Society, Washington, DC, 1994), Ch. 4, p. 39.

[24] H. Ohtsuka and T. Tabata, Appl. Catal. B 21 (1999) 133.

[25] R. Van Hardeveld and H.H. Artog, Surface Sci. 15 (1969) 189.